

Clinical trial of a farnesyltransferase inhibitor in children with Hutchinson–Gilford progeria syndrome

Leslie B. Gordon^{a,b,c,1,2}, Monica E. Kleinman^{a,b,1}, David T. Miller^{d,e,f,1}, Donna S. Neubergh^{g,h}, Anita Giobbie-Hurder^g, Marie Gerhard-Hermanⁱ, Leslie B. Smoot^j, Catherine M. Gordon^{c,k,l}, Robert Cleveland^m, Brian D. Snyder^{n,o}, Brian Fligor^p, W. Robert Bishop^q, Paul Statkevich^q, Amy Regen^r, Andrew Sonis^r, Susan Riley^s, Christine Ploski^s, Annette Correia^s, Nicolle Quinn^{t,u}, Nicole J. Ullrich^v, Ara Nazarian^o, Marilyn G. Liang^{d,w}, Susanna Y. Huh^{d,u}, Armin Schwartzman^{g,h}, and Mark W. Kieran^{x,y,2}

Departments of ^aAnesthesia, ^dMedicine, ^eLaboratory Medicine ^lCardiology, ^mRadiology, ⁿOrthopedics, ^pOtolaryngology and Communication Enhancement ^tDentistry, ^uPhysical Therapy and Occupational Therapy Services, and ^vNeurology Boston Children's Hospital and Harvard Medical School, Boston, MA 02115; Divisions of ^bCritical Care Medicine, ^cGenetics, ^kAdolescent Medicine, ^hEndocrinology, ^gGastroenterology and Nutrition, ^wDermatology, and ^sHematology-Oncology, Boston Children's Hospital and Harvard Medical School, Boston, MA 02115; ^qDepartment of Pediatrics, Hasbro Children's Hospital and Warren Alpert Medical School of Brown University, Providence, RI 02903; ⁹Department of Biostatistics and Computational Biology, Dana-Farber Cancer Institute, Boston, MA 02215; ¹⁰Department of Biostatistics and Harvard School of Public Health, Boston, MA 02115; ¹¹Department of Medicine, Cardiovascular Division, Brigham and Women's Hospital, Harvard Medical School, Boston, MA 02115; ¹²Merck Research Laboratories, Kenilworth, NJ 07033; ¹³Clinical Translational Study Unit, Boston Children's Hospital, Boston, MA 02115; ¹⁴Center for Advanced Orthopaedic Studies, Department of Orthopaedics, Beth Israel Deaconess Medical Center and Harvard Medical School, Boston, MA 02115; and ¹⁵Division of Pediatric Oncology, Dana-Farber Cancer Institute, Boston, MA 02215

Edited* by Francis S. Collins, National Institutes of Health, Bethesda, MD, and approved August 13, 2012 (received for review February 16, 2012)

Hutchinson–Gilford progeria syndrome (HGPS) is an extremely rare, fatal, segmental premature aging syndrome caused by a mutation in *LMNA* that produces the farnesylated aberrant lamin A protein, progerin. This multisystem disorder causes failure to thrive and accelerated atherosclerosis leading to early death. Farnesyltransferase inhibitors have ameliorated disease phenotypes in preclinical studies. Twenty-five patients with HGPS received the farnesyltransferase inhibitor lonafarnib for a minimum of 2 y. Primary outcome success was predefined as a 50% increase over pretherapy in estimated annual rate of weight gain, or change from pretherapy weight loss to statistically significant on-study weight gain. Nine patients experienced a $\geq 50\%$ increase, six experienced a $\geq 50\%$ decrease, and 10 remained stable with respect to rate of weight gain. Secondary outcomes included decreases in arterial pulse wave velocity and carotid artery echodensity and increases in skeletal rigidity and sensorineural hearing within patient subgroups. All patients improved in one or more of these outcomes. Results from this clinical treatment trial for children with HGPS provide preliminary evidence that lonafarnib may improve vascular stiffness, bone structure, and audiological status.

SCHE6336 | laminopathy | cardiovascular disease | translational medicine

Hutchinson–Gilford progeria syndrome (HGPS) is an autosomal dominant, rare (incidence 1 in 4 million live births), fatal pediatric segmental premature aging disease for which there is no known treatment (1). Classic HGPS is caused by a single base mutation, c.1824C > T, in *LMNA* (2, 3) activating an alternative splice site to produce an abnormal lamin A protein named “progerin.” Lamin A, an inner nuclear membrane protein, broadly influences nuclear structure and function (4). Progerin lacks the proteolytic cleavage site normally used to remove the farnesylated carboxy terminus from lamin A during posttranslational processing (3). Persistent farnesylation causes progerin accumulation in the inner nuclear membrane and is at least partly responsible for the HGPS phenotype (5). Disease manifestations include severe failure to thrive, scleroderma-like skin, lipatrophy, alopecia, joint contractures, skeletal dysplasia, and atherosclerosis, but intellectual development is normal (6). Death at an average age of 13 y occurs from myocardial infarction or stroke (7).

Farnesyltransferase inhibitors (FTIs) are small molecules which reversibly bind to the farnesyltransferase CAAX binding site (8), thereby inhibiting progerin farnesylation and intercalation into the nuclear membrane. Cultured progerin-containing cells normalize both structure and function when treated with FTIs (reviewed in ref. 9). In transgenic HGPS murine models treated with FTIs, cardiovascular defects (10), bone mineralization, and weight are improved, and lifespan is extended (11).

Given the 100% fatality rate in HGPS, promising preclinical studies with FTIs, and the favorable side-effect profile of the FTI lonafarnib in the pediatric non-HGPS population (12), we initiated a prospective single-arm clinical trial. We previously demonstrated that children over age 2 y with HGPS have a linear rate of weight change which remains consistent within each child over time, unaffected by age or puberty (13). Each child exhibits a very low maximum rate of weight gain despite a normal caloric intake (6). Rate of weight gain differs among children but is very stable within a given child. Our initial hypothesis was that each child with HGPS has his or her own physiological, disease-related “ceiling” in his or her rate of weight gain and would be unable to increase the rate of weight gain without treatment of the disease. Multiple other disease measures were assessed as secondary outcomes. We now report on outcome and toxicity data from 25 children with HGPS [75% of the known worldwide population at trial initiation (14)] who were treated with lonafarnib for at least 2 y.

Results

Patients. Twenty-six patients with classic HGPS from 16 countries were enrolled in this phase II clinical trial of lonafarnib from May through October 2007. One child with a history of prior strokes died of a stroke after 5 mo on study. Therefore, results are reported as pharmacokinetics (PK) and toxicity for the 26 patients treated at the 115 mg/m² dose and as PK, toxicity, and outcome for the 25 patients who completed at least 2 y of therapy. Pretherapy patient characteristics (Table 1) were similar to previously reported data (6, 15, 16). Two additional patients had nonclassic mutations and are not included in this analysis.

Author contributions: L.B.G., M.E.K., D.T.M., D.S.N., A.G.-H., and M.W.K. designed research; L.B.G., M.E.K., D.T.M., M.G.-H., L.B.S., C.M.G., R.C., B.D.S., B.F., A.R., A. Sonis, S.R., C.P., A.C., N.Q., N.J.U., A.N., M.G.L., S.Y.H., and M.W.K. performed research; W.R.B. and P.S. contributed new reagents/analytic tools; L.B.G., M.E.K., D.T.M., D.S.N., A.G.-H., M.G.-H., W.R.B., P.S., A. Schwartzman, and M.W.K. analyzed data; and L.B.G., M.E.K., D.T.M., D.S.N., A.G.-H., M.G.-H., L.B.S., C.M.G., R.C., B.D.S., B.F., A.R., A. Sonis, S.R., C.P., A.C., N.J.U., A.N., M.G.L., S.Y.H., and M.W.K. wrote the paper.

Conflict of interest statement: W.R.B. and P.S. are employees of Merck Pharmaceutical, the company that supplied the experimental agent for this clinical trial. L.B.G. is the mother of a child with progeria who participated in this study.

*This Direct Submission article had a prearranged editor.

Freely available online through the PNAS open access option.

¹L.B.G., M.E.K., and D.T.M. contributed equally to this work.

²To whom correspondence may be addressed. E-mail: Leslie_Gordon@brown.edu or mark_kieran@dfci.harvard.edu.

This article contains supporting information online at www.pnas.org/lookup/suppl/doi:10.1073/pnas.1202529109/-DCSupplemental.

Table 1. Patient characteristics at study entry

Characteristic	Mean	S.D.	Minimum	Median	Maximum
Age at enrollment (y)	7.0	3	3	7	16
Height-age (y)	3.4	1.6	1.0	3.0	7.0
Weight (kg)	10.4	2.7	6.6	9.5	17.6
Standing height (cm)	94.9	11.9	76.7	93.8	122.0
Standing height BMI	11.4	1.2	9.3	11.7	13.5
Z-scores for standing height*	-5.41	1.33	-7.34	-5.43	-3.47
Z-scores for weight*	-10.18	5.90	-33.69	-9.04	-5.30

Of the 25 participants, 11 (44%) were male, and 14 (56%) were female. *Derived from age- and sex -adjusted reference values using 2000 Centers for Disease Control Growth Charts (41).

One additional patient signed consent but withdrew from the protocol before receiving therapy.

Lonafarnib Treatment. Overall, therapy was well tolerated, and no child came off study because of toxicity. Twenty-four of 26 children tolerated the 150 mg/m² dose. One patient escalated from 115 mg/m² to 150 mg/m² and then de-escalated to 115 mg/m² because of brawny edema in the perineal region; although of unknown etiology, this finding was present only at the higher dose. One patient experienced increased bowel gas, vomiting, and gastric pain even when de-escalated to 115 mg/m². After a 2-wk lonafarnib holiday, drug was restarted at 115 mg/m² and was well tolerated and then was escalated to 150 mg/m² for the remainder of the trial. Generally, drug-related side effects included mild diarrhea, fatigue, nausea, vomiting, anorexia, and depressed serum hemoglobin. Toxicity details, presented in Table S1, are consistent with the known toxicity profile of this agent (12) and improved over time for most patients.

Changes and Key Factors in Rate of Weight Gain. Our a priori statistical design required 3 of the 25 enrolled patients to attain a >50% increase in slope for weight gain or a change from negative to positive slope. Nine of 25 patients [36%; 95% exact binomial confidence interval (CI): 18–58%] achieved success (Fig. 1). Sixteen patients experienced a rate of weight change on study that was <50% increased from the rate before study entry; 10 had stable rates ($\pm 50\%$), and six had decreases of >50%. The rates of weight gain on study experienced by the nine patients were statistically greater than zero; the rates of weight gain on study in the six patients did not differ from zero. Of note, the four patients whose rates before study entry were negative (-0.552, -0.444, -0.084, and -0.036 kg/y) attained statistically significant rates of weight gain on therapy (0.410, 0.574, 1.331, and 0.462 kg/y, respectively).

We assessed factors that may have contributed to rate of weight gain success vs. nonsuccess (Table 2 and Table S2). It appears that weight gain from muscle ($P = 0.005$) and bone ($P = 0.04$), but not fat ($P = 0.78$), accounted for success. Because dual X-ray absorptiometry (DXA) cannot differentiate fat within the lean compartment (17), and fat infiltration would result in muscle weakening, we measured quadriceps muscle strength. There was no evidence of weakening for the overall patient group or within the weight gain success and nonsuccess groups. (Table S2).

Patient age, sex, and energy balance did not contribute to lonafarnib's effect (Table 2 and Table S2). Caloric intake for all patients was sufficient for growth [$\geq 90\%$ of the recommended dietary allowance (RDA) for age] at both study entry and at end of therapy. At both time points, measured resting energy expenditure (MREE) was either well below or within 10% of that predicted ($n = 24/25$) (18). Only one patient had an MREE that was 120% of predicted.

Cardiovascular Changes. At pretherapy, the carotid-femoral pulse wave velocity (PWV_{cf}) in 18 subjects was 3.5 times greater than the established pediatric normal values (16, 19), indicating high arterial stiffness and low distensibility (median: 12.9 m/s; range:

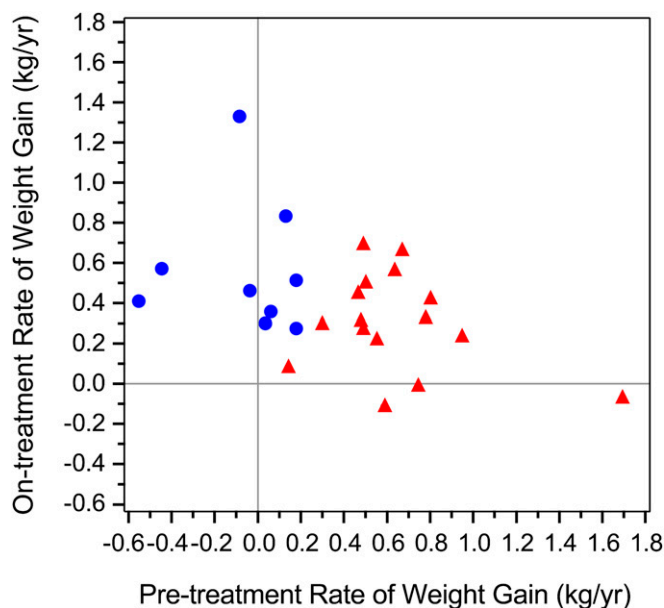


Fig. 1. Effect of lonafarnib on body weight. Pretherapy rate of weight change (x axis) vs. on-therapy rate of weight change (y axis) in 25 trial participants. Blue circles, 50% increase in rate of weight gain (success) ($n = 9$). Red triangles, <50% increase in rate of weight gain (lack of success) ($n = 16$).

7.2–18.8 m/s) (Fig. 2) (20). At end of treatment, PWV_{cf} decreased by a median of 35% (range: 48% decrease to 26% increase, $P = 0.0001$) with a median observed change in PWV_{cf} (post- vs. pretreatment) of -4.5 m/s (range: -7.4m/s to 1.9 m/s). Published normal values encompass ages ≥ 7 y (16, 19); in our study, there was no difference in results when we included only patients ≥ 7 y old. Two patients taking an angiotensin-converting enzyme inhibitor or calcium-channel blocker had PWV_{cf} data similar to those not taking antihypertensive medications.

Carotid arteries demonstrated greater wall echodensity at the intima media and near adventitia in HGPS patients than in age- and sex-matched controls (Fig. S1, Table 3, and Table S3) (16). This finding likely represents an underestimation of pretherapy abnormality because of saturation of the upper limit of grayscale detection (Fig. S1G). Echodensity of the intima media and near and deep adventitia decreased with lonafarnib treatment (Table 3 and Table S3). At the end of therapy, the echodensity of the intima media and near adventitia in the HGPS cohort was not different from that of controls. The deep adventitia was less echobright than in controls at the end of therapy. Median carotid intima media thickness was normal both pretherapy (0.42 mm

Table 2. Rate of weight gain

	Weight gain end point			
	Achieved ($n = 9$)*		Not achieved ($n = 16$)*	
	Median	Range	Median	Range
Rate of weight gain (kg/y)				
Pretreatment	0.04	-0.55–0.18	0.57	0.14–1.69
Posttreatment	0.52	0.14–1.33	0.31	-0.53, 0.70
Fold change	5.98	0.75–25.50	0.57	-1.07, 1.42
Demographics				
Age at study entry (y)	4.8	3.3–10.9	8.8	3.1–16.2
Percent male	44.4		43.8	

*One patient in the achieved group and four patients in the not-achieved group received recombinant growth hormone therapy.

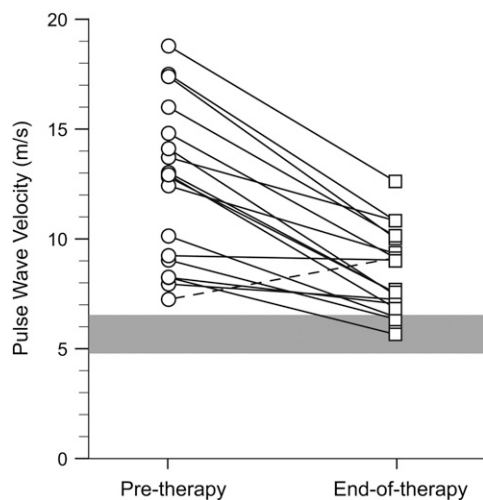


Fig. 2. PWV improvements with lonafarnib therapy. PWV_{cr} in m/s (y axis) for each trial participant at pretherapy (circles) and end of therapy (squares); connecting lines show change in PWV for each child ($n = 18$). Published normal range (4.8–6.6 m/s) (23) is plotted as a solid horizontal blue bar for comparison. All participants except one (dashed line) showed improvement in PWV.

bilaterally) and at end of- herapy (right = 0.41 mm; left = 0.42 mm) (6, 16).

Changes in Skeletal Rigidity and Areal Bone Mineral Density. Our previously reported peripheral quantitative CT (pQCT) studies demonstrated that resistance of the metaphysis and diaphysis of the radius to compressive, bending, and torsional loads is severely abnormal in HGPS (15). Lonafarnib treatment led to median percent increases at the four radial sites tested of 40–50% in axial rigidity, 170–228% in flexural rigidity, and 167–229% in torsional rigidity (Fig. 3 and Fig. S2) in the subset of 11 patients who could be tested, achieving values equivalent to age- and sex-matched controls ($n = 55$ –58). The 20%, 50%, and 66% radial sites showed similar findings (Fig. S2).

Strength strain index (SSI), an estimate of bone bending strength, showed median increases of 9% (range: 17% decrease to 193% increase) at the 20% site ($n = 22$; $P = 0.002$), 35% (range: 3% decrease to 138% increase) at the 66% site ($n = 10$; $P = 0.01$), and 9% (range: 13% decrease to 30% increase) at the 50% site ($n = 13$; $P = 0.06$).

Areal bone mineral density (aBMD) demonstrated a clinically significant $\geq 3\%$ increase from pretherapy to end of therapy at one or more sites in 76% of children (19/25; exact 95% CI: 55–91%) compared with 40% of the participants (10/25; exact 95% CI: 21–61%) who exhibited decreases at one or more sites (Fig. S2). Seven children experienced both clinically significant losses and gains at different sites. Two children had improvements in all three measured sites: total body, hip, and spine. Ten children had improvements in two of three sites, and seven had improvements in one site only. See Table S4 for detailed aBMDs.

Mean serum total protein, calcium, vitamin D, and phosphorous were normal pretherapy and at end of therapy, as was radius volumetric bone mineral density (vBMD) (15) assessed by pQCT. Fracture incidence was 3/25 children pretherapy and 2/25 children during therapy.

Audiological Changes. Sensorineural hearing was in the normal or low-normal range in both ears for all assessable patients at study initiation. At end of study, median low-frequency sensorineural hearing improved in both the better-hearing ear ($n = 18$; $P = 0.008$) and the poorer-hearing ear ($n = 16$; $P = 0.002$) (Fig. S3). Clinically, 8/18 children, representing 13/34 ears, experienced ≥ 10 dB improvement in average low-frequency sensorineural hearing (44%; 95% exact CI: 22–69%). Median high-frequency sensorineural hearing, assessable in only five patients, was unchanged in both ears. Conductive hearing was largely unchanged by treatment (SI Results, Audiology Results). Speech reception/awareness thresholds corroborated tonal findings, and word recognition scores were 96–100% for all patients tested.

Lonafarnib Pharmacokinetics. PK characteristics were similar to those previously published in non-HGPS pediatric patients (12). Median time to maximum drug concentration was 2 h at 115 mg/m² ($n = 24$) and 4 h at 150 mg/m² ($n = 21$), with dose-related increases in maximum concentration and area under the curve (Table S5 and Fig. S44). Lonafarnib was absorbed and eliminated slowly over a 12-h period, with predose steady-state concentrations of 45% and 51% of maximum concentration values for 115 mg/m² and 150 mg/m², respectively.

Pharmacodynamics. Patient blood samples (provided pretherapy, at week 52, and at end of therapy) were analyzed for inhibition of HDJ-2 farnesylation (Fig. S4B). Fifty-two percent (13/25) displayed inhibition (range, 10.2–35.7%) at one or both on-therapy time points (Table S6). However, 6 of these 13 patients (46%) showed inhibition of HDJ2 farnesylation at week 52 but not at the end of therapy. Whenever possible, this lack of farnesylation inhibition was confirmed by repeat analysis of the sample. Although six of nine subjects with positive weight gain demonstrated HDJ-2 shifts in at least one time point, 9 of 16 subjects without improvement in rate of weight gain also had shifts in HDJ-2 (Fisher’s exact P value 0.69) (Fig. S4C). For comparison, new data are presented from a study of lonafarnib treatment of chronic myelomonocytic leukemia and myelodysplastic syndrome cancers showing longitudinal data on HDJ-2 inhibition (SI Results, Pharmacodynamics) (21).

Pertinent Negatives. Several measures that were abnormal pretherapy did not change significantly with treatment. These included ECG and several carotid ultrasound findings (SI Results), joint contractures (6), X-ray findings (13), and dental abnormalities (22). Serum leptin levels were below the lower limit of detection (<0.5 ng/L) at both study pretherapy and end of therapy for 13 of 25 children (52%), and only one child had detectable levels of serum leptin at both times, reflecting persistently low levels of adipose tissue. The rate of insulin resistance was similar at study entry (8/24 children; 33.3%) and at

Table 3. Effect of lonafarnib on carotid artery density by ultrasound

Site	Percentile	Median density in pixels (range)			P value		
		Control ($n = 55$)	HG(P) ($n = 22$)	HG(E) ($n = 22$)	Control vs. HG(P)*	HG(P) vs. HG(E) [†]	Control vs. HG(E)*
Intima media	50	73.0 (28.0–156.0)	87.0 (15.0–242.0)	72.0 (2.0–140.0)	0.002	0.002	0.75
Adventitia luminal near wall	50	169.0 (95.0–237.0)	228.0 (61.0–254.0)	170.0 (70.0–252.0)	0.0004	0.003	0.46
Adventitia deep near wall	50	166.0 (34–254.0)	167.0 (30.0–254.0)	121.0 (12.0–215.0)	0.32	0.05	0.002

HG(E), HGPS end of therapy; HG(P), HGPS pretherapy.

*Based on Wilcoxon rank-sum test.

[†]Wilcoxon signed-rank test based on distributions of fold-change (post-/pre-treatment) calculated for each patient.

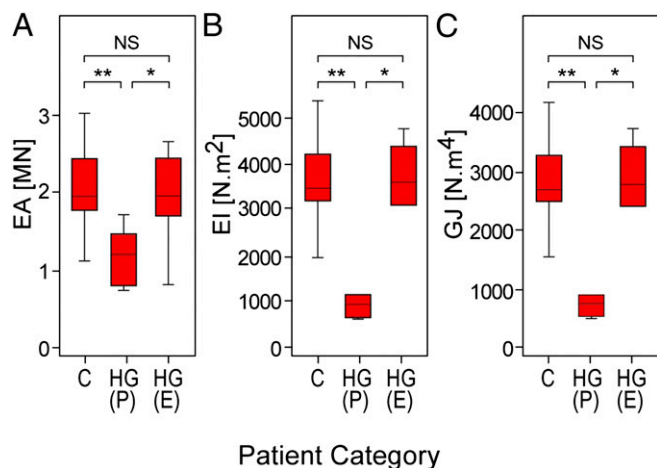


Fig. 3. Lonafarnib normalized skeletal rigidity in HGPS. Box plots of (A) cross-sectional axial (EA), (B) bending (EI), and (C) torsional (GJ) rigidities measured using pQCT at the fourth percentile radial site in control (C), HGPS pretherapy [HG(P)], and HGPS end-of-therapy [HG(E)] groups. We published this control group's data previously (15) and include it here for statistical comparison with the HGPS groups. Top and bottom box edges represent the 75th and 25th interquartile (IQR) ranges, respectively. Horizontal lines within boxes represent medians. Lower and upper whiskers represent $Q1 - 1.5 \times IQR$ and $Q3 + 1.5 \times IQR$. * $P < 0.01$; ** $P < 0.001$; NS, $P > 0.05$.

end of therapy (9/24 children; 37.5%). Hair counts by dermatologic assessment were unchanged pre- vs. end of therapy.

Associations. No associations between age at time of treatment and outcome measures that were improved at end of study (rate of weight gain, PWV_{cf} , echodensity, aBMD, pQCT-derived structural rigidities, and audiology) were identified.

Discussion

We report results from the initial clinical treatment trial for children with HGPS. For some patients, lonafarnib therapy increased the rate of weight gain and improved measures of cardiovascular stiffness, bone structure, or audiological status. Every child completing the study showed improvement in one or more of these categories. Although we did observe increases between the pre- and posttherapy rates of weight gain in a number of patients, the rate of weight gain in all patients remained significantly lower than norms based on patient age. The increased rate of weight gain was attributable to increased lean body mass and bone and was not associated with increased caloric intake, changes in intestinal absorption, or changes in energy expenditure (6). Although nine patients increased their rates of weight gain increased by $\geq 50\%$, six patients' rates of weight gain decreased by $\geq 50\%$. Possible causes for a decreased rate of weight gain include intolerance to medication, progression of disease, and rigor of travel and testing procedures. The four patients with negative weight gain slopes at trial entry attained among the steepest on-treatment slopes, whereas those who entered the trial with the highest rates of weight gain tended to decrease their rates of weight gain. These results generate a hypothesis that the children who had low or negative rates of weight gain before treatment benefited with respect to rate of weight gain, whereas some who had higher rates of weight gain before treatment did not benefit or may have been affected adversely with respect to rate of weight gain. This hypothesis will need to be tested in future trials.

Lonafarnib therapy resulted in evidence for the improved cardiovascular status of children with HGPS, a potentially important finding because failure of this organ system is the ultimate cause of mortality. Treatment improved peripheral arterial stiffness, reflected by highly elevated pretherapy PWV (the accepted standard measure of vascular stiffness) and echodense common carotid arteries (16). In a study of baseline values for

PWV in 1,008 healthy children ages 7–19 y, Reusz et al. (19) found decreases in normal values with decreasing age and height. The PWV values for children in these age ranges, with sex, age, and height charts all considered, are between 3.368 and 4.528 at the fifth percentile, 4.269 and 5.713 at the 50th percentile, and 5.231 and 7.288 at the 95th percentile. Although there are no established norms for children below age 7 y, we would expect the PWV for normal subjects under age 7 y to be at least as low as that of a 7-y-old child. In addition, there are no published pediatric data that determine the clinical benefit of decreasing an elevated PWV toward normal; we must extrapolate from adult data to hypothesize that decreasing vascular stiffness may benefit the HGPS pediatric population. Statistical significance between pretherapy and end-of-therapy PWV was present both in patients under age 7 y and in those age 7 y and older.

In the general population, aortic stiffness is an independent predictor of cardiovascular and stroke mortality as well as of nonfatal coronary events (reviewed in ref. 23). Arterial stiffness normally increases with age, and although our HGPS cohort initially exhibited PWV equivalent to the age range of 60–69 y, median end-of-therapy PWV was in the range of a typical 40- to 49-y-old (24). Based on studies of non-HGPS patients with diabetes, where aortic PWV increments as small as 1 m/s have a significant independent effect on reduced mortality (25), the median 4.5-m/s decrease detected in our study implies a potential for benefit to cardiovascular mortality in children with HGPS.

We detected abnormally high adventitial echobrightness consistent with previous reports in an HGPS mouse model (26) and in HGPS patients (16, 27). Interpretation of echobright signal with carotid ultrasound is a less-established measure of arterial wall density (28). However, autopsy examination has identified abnormally dense and ECM-rich intima media and adventitia (27, 29). Given these findings, we speculate that the abnormal ECM contributes to vascular stiffness in HGPS patients, and the evidence for improvement in structure (reflected by echodensity) and function (reflected by PWV) are encouraging with regard to possible alteration of the progressive vascular aspects of this disease.

Quantifiable, consistent vascular abnormalities are crucial to the study of HGPS, because death is caused by cerebro- and cardiovascular events. Our results suggest that lonafarnib treatment results in positive effects on the cardiovascular system in children with HGPS. Given that these cardiovascular abnormalities were first quantified within the context of this trial, and given that only subgroups of the trial cohort could perform the studies successfully, it will be important to continue to evaluate the potential cardiovascular benefit in future clinical treatment trials.

To explore skeletal changes, we used both the traditional bone assessment tool, DXA, and pQCT. Although the change in aBMD suggests that with treatment there may have been an increase in bone mass at various sites, it is not possible to know by this method if these findings represent an improvement over the expected aBMD decline with time in this population, where bone geometry is strikingly abnormal (15).

Unlike DXA which measures the aBMD over a specified region of analysis (integrating both the mineralization of the bone and its out-of-plane width in a single parameter), pQCT specifically measures the vBMD and 3D geometry of the bone, independent of patient size (30). Treatment with lonafarnib resulted in evidence for improved material, geometric, and structural parameters contributing to bone strength. Measures of structural rigidity integrating bone stiffness and cross-sectional geometry to resist axial (EA), bending (EI), and torsional (GJ) loads were well below those in our normal control group before therapy and achieved normal values at end of therapy. Increased SSI pQCT data suggest that there was an increase in the diameter of the bone by periosteal expansion. Overall, the changes in bone structure reflect improvements in bone geometry so that the bone could support more load and therefore was expected to be more fracture-resistant.

Although some laminopathies exhibit neurologic deficits, neuropathology is not classically noted in HGPS other than deficits caused by stroke (31). However, we found that low-frequency sensorineural hearing, which is dependent on neurological status,

was improved at end of therapy. Conductive hearing, which is dependent on structural components of the outer and/or middle ear and classically is affected in HGPS, was largely unchanged. This finding could indicate that there are subtle neurologically based findings in HGPS that have not been detected in prior studies or that lonafarnib affects neurological hearing through a target protein other than progerin.

We chose a single-arm study design. First, HGPS, although genetically uniform, has wide range of clinical severity at any given age. There is no validated disease severity score, and age matching would not be an effective way to pair cases vs. controls. Additionally, our pretrial clinical data on rate of weight gain showed that, although interpatient rates of weight gain vary widely, inpatient rates are extremely consistent after age 2 y (13). Thus, each child served as his or her own control for the primary outcome measure, and this consistency lent itself well to a single-arm design. Finally, given the 100% mortality rate in HGPS, we designed a trial that would allow all patients to receive potential therapy.

We note several study limitations. Although we included 75% of identified cases at the time of trial entry and an estimated 13% of the world's HGPS population, we were limited by both the total size of our cohort (25 patients) and the number of children who could not adequately perform various tests because of age or fragility. Furthermore, because of the rarity of this disease, very little comprehensive longitudinal data were available at the time of study development, limiting our choice of primary outcome measures as well as our ability to detect dampened disease progression. Hence, aside from rate of weight gain, demonstrating lonafarnib efficacy required that we both identify clinical abnormalities that are exhibited consistently and measured objectively and also that we detect reversal of abnormalities rather than lack of disease progression. The abnormalities we identified were PWV, echodensity, SSI, and structural rigidity, which we hope will be instrumental in guiding outcome measures for future intervention studies. Finally, despite a number of interim clinical markers that demonstrated improvement with lonafarnib therapy, true clinical impact measured by decreased morbidity and improved survival was not assessable in our limited 2-y time frame.

We found a lack of correlation between the pharmacodynamic marker used and clinical response. This finding is commensurate with previous findings in cancer studies that also used HDJ-2 as a potential surrogate marker of farnesylation inhibition. Findings were similar for range of inhibition (12), variable longitudinal inhibition, and lack of clear association with clinical outcomes (21). Although HDJ-2 assessment confirms on-target biochemical activity of lonafarnib in a subset of patients, it does not provide a useful biomarker for predicting clinical benefit. The lack of correlation between unfarnesylated HDJ-2 and clinical benefit may be attributable, at least in part, to the use of a surrogate farnesylated protein in a surrogate tissue. Different farnesyltransferase substrates show differing sensitivities to the effect of CAAX-competitive FTIs, depending on their intrinsic affinity for the enzyme (32). Given the limitations of assessing HDJ-2 farnesylation, it may be valuable to develop methodologies that allow a direct assessment of the farnesylation status of progerin in patient-derived samples in future clinical studies. Although progerin and lamin A can be obtained from skin biopsies (27, 33), no study has tested a correlation between farnesylation inhibition and extent of improvement in HGPS mouse model studies of FTI, and, without strong preclinical support, serial biopsies in children are unethical. Although currently unavailable, if measuring progerin and progerin farnesylation status from blood samples or buccal smears becomes technically reliable, correlations with clinical efficacy should be tested rigorously in preclinical mouse studies, because tissue penetration and cell type susceptibility to the damaging effects of progerin vary widely in different organ systems in HGPS.

Our results have a number of implications beyond HGPS. Progerin, the disease-causing protein in HGPS, is also produced in normal individuals and increases with age (27, 34, 35). A number of studies have linked progerin with normal senescence, including a causal link with telomere dysfunction in senescence

(36). Hence, continued research into how progerin and the application of FTIs to generalized aging and cardiovascular disease will likely prove informative (27, 35–37). Importantly, this trial demonstrates the potential of translating basic biomedical and genetics research into human treatment. Therapy stemming from the discovery of the HGPS gene mutation in 2003 (2, 3) was supported by decades of basic research into the biology and posttranslational processing of lamin A used to generate the hypothesis that farnesylation inhibition might be useful in HGPS. Repurposing of lonafarnib, a drug in advanced stages of development for cancer, ensued. Proof-of-principle treatment with FTI both in vitro (reviewed in ref. 9) and in newly created HGPS mouse models followed (10, 38). This study brings these remarkable preclinical efforts to human application.

Materials and Methods

Participants were ≥ 3 y of age with clinically and genetically confirmed c.1824 C > T, p. Gly608Gly classic HGPS and adequate organ and marrow function and were able to travel for regular study visits. Participants also had pretrial weights (including at least five data points) obtained at intervals of at least 1 mo during the year before study entry. All parents or legal guardians provided written informed consent that was approved by the Boston Children's Hospital Committee on Clinical Investigation. Consents were translated into the parent(s)' primary language, and discussions were performed with interpreters. Assent was obtained from children old enough to comprehend. The study is registered with [Clinicaltrials.gov](https://www.clinicaltrials.gov) (NCT00916747). All measures reported were designed before study initiation and were included as part of the trial protocol. Most pretrial clinical information and weights were obtained from The Progeria Research Foundation Medical and Research Database, with parental consent (www.progeriaresearch.org/medical_database.html) as previously described (13). For some patients, clinical information and weights were provided directly by the referring physicians. On-study histories and physicals and all efficacy testing were performed at Boston Children's Hospital or Brigham and Women's Hospital, Boston, MA. Insulin resistance (IR) was determined using homeostasis model assessment-insulin resistance (HOMA-IR) index = fasting (glucose) \times (insulin)/405. A HOMA-IR index ≥ 2.5 denotes insulin resistance.

Dosage and Administration. Lonafarnib (Merck & Co., Inc.) dosing was initiated at 115 mg/m² and was increased to 150 mg/m² after an adjustment period of at least 4 mo. Dosage was reduced back to 115 mg/m² for patients experiencing drug-related grade 3 or 4 toxicity and also not responding to supportive care. Once dosage was reduced, patients were permitted to increase the dose of lonafarnib. Patients received oral lonafarnib either by capsule or liquid suspension dispersed in Ora-Blend SF or Ora-Plus (Paddock Laboratories, Inc.) every 12 \pm 2 h for a period of 24–29 mo. Patients were monitored for liver, kidney, and hematological toxicity each month for the first 3 mo by their local physicians and every 4 mo in Boston for the duration of the study. Adverse events were monitored and recorded throughout the study.

Annual Rate of Weight Gain. Because children with HGPS have linear and individualized maximal rates of weight gain that remain stable over time (13), primary outcome success was predefined as a 50% increase over pretherapy in estimated annual rate of weight gain or as a change from pretherapy weight loss to a statistically significant on-study weight gain. This method allowed each patient to act as his or her own control, with his or her own rate of weight gain pretherapy compared with his or her own rate on-therapy. With this design in mind, a weighing program was used during the year before trial initiation for the majority of patients who planned to join the trial, through The Progeria Research Foundation Medical and Research Database. Most families were sent a scale and instructions in language of origin, and the participant was weighed weekly, before breakfast, wearing underwear. Several children's pretrial weights were reported through home physicians.

Pretrial rate of weight gain was estimated using least squares regression for the prior year's data available at study entry. A separate analysis was performed with the seven measurements obtained on study at Boston Children's Hospital using the same methodology. Statistically significant weight change was defined as rate of weight change estimated by the slope in the least squares regression and tested at the 0.05 level by the *t* test.

Our trial design, based on 25 patients, required that three or more patients achieve improvement in the rate of weight gain (defined as at least a 50% increase in the annual rate of weight gain). Such a result would rule out a null hypothesis of weight gain improvement in 5% of patients at a 0.13 one-sided

significance level and would have 97% power to detect a rate of weight gain improvement in 25% of patients.

Nutrition, Cardiovascular, Skeletal, and Audiologic Testing. Nutrition, cardiovascular, and skeletal analysis and audiologic methods are described in *SI Methods*.

Nutrition was assessed using daily caloric intake calculated from 7-d food records, using the nutrient analysis program Nutrition Data System for Research (University of Minnesota, Minneapolis, MN). MREE was obtained using the V_{\max} 29N indirect calorimetry cart (CareFusion, San Diego, CA) after a minimum 4-h fast.

For cardiovascular testing, fasting PWV_{cf}, diagnostic carotid artery ultrasonography, mean distal internal carotid artery velocity, distal common carotid artery far-wall intima media thickness, and echodensity procedures were performed as previously described (16). Quantification of ultrasound images was performed in a blinded fashion.

For skeletal analysis, DXA of the lumbar spine, total hip, and whole body were performed as previously described (15). Clinically significant improvement in aBMD was predefined as a $\geq 3\%$ increase (39). vBMD, SSI, and load-bearing capacity [axial (EA), bending (EI), and torsional (GJ) rigidities] were calculated by a technician who was blinded to identifiers, using pQCT images obtained at serial cross-sections through the radius. These rigidity values reflect the structural properties of the cancellous and cortical bones at 4%, 20%, 50%, and 66% distances.

For audiologic testing, sensorineural and conductive hearing status were assessed by bone and air conduction, respectively. Low-frequency hearing loss was defined as hearing thresholds > 15 dB averaged over 250, 500, and 1,000 Hz. High-frequency hearing loss was comparably defined over 2,000, 4,000, and 8,000 Hz. Clinically significant change was predefined as a difference of ≥ 10 dB, averaged across the three frequencies (40).

Statistics. The primary end point of the study was improvement in rate of weight gain: either a rate of weight gain on study that was 50% higher than the rate estimated before study entry or a transition from a pretherapy estimated weight loss to a statistically significant weight gain on study. All rates of weight change were estimated by the slope of a patient-specific least squares regression using data collected within the year before study entry and data collected during therapy. With 25 patients, the study would have 90% power to detect a 25% rate of weight gain improvement, compared with a null of 5%, using a 0.127 one-sided significance level. Exact binomial calculations were used in planning the study and in providing the 90% CI for the primary outcome measure. Per protocol, 90% exact binomial CIs were planned a priori and are provided in *SI Results*; 95% CIs reflect a post hoc analysis. To identify the parameters that might be useful as end points in future studies, *P* values using the Wilcoxon signed-rank test were provided for secondary and exploratory end points. These *P* values do not reflect adjustment for multiple comparisons and should be interpreted only descriptively. Comparisons of study subjects with age-matched controls recruited for selected bone and cardiovascular measures were conducted using the Wilcoxon rank-sum test. Relationships between outcomes and age were assessed using Spearman's correlations.

ACKNOWLEDGMENTS. Most importantly, we are grateful to the children with progeria and their families and to the children who participated as control subjects for participation in this study. Additional acknowledgments are included in *SI Results*. This project was funded by Grant PRFCLIN2007-01 from The Progeria Research Foundation, by the Dana-Farber Cancer Institute Stop & Shop Pediatric Brain Tumor Program, the C.J. Buckley Fund, the Kyle Johnson Fund, and by the National Center for Research Resources, National Institutes of Health Grants MO1-RR02172 to the Boston Children's Hospital General Clinical Research Center and UL1 RR025758-01 to the Harvard Catalyst Clinical and Translational Science Center.

1. Kieran MW, Gordon L, Kleinman M (2007) New approaches to progeria. *Pediatrics* 120:834–841.
2. De Sandre-Giovannoli A, et al. (2003) Lamin A truncation in Hutchinson-Gilford progeria. *Science* 300:2055.
3. Eriksson M, et al. (2003) Recurrent de novo point mutations in lamin A cause Hutchinson-Gilford progeria syndrome. *Nature* 423:293–298.
4. Broers JL, Ramaekers FC, Bonne G, Yaou RB, Hutchison CJ (2006) Nuclear lamins: Laminopathies and their role in premature ageing. *Physiol Rev* 86:967–1008.
5. Goldman RD, et al. (2004) Accumulation of mutant lamin A causes progressive changes in nuclear architecture in Hutchinson-Gilford progeria syndrome. *Proc Natl Acad Sci USA* 101:8963–8968.
6. Merideth MA, et al. (2008) Phenotype and course of Hutchinson-Gilford progeria syndrome. *N Engl J Med* 358:592–604.
7. Hennekam RC (2006) Hutchinson-Gilford progeria syndrome: Review of the phenotype. *Am J Med Genet A* 140:2603–2624.
8. Basso AD, Kirschmeier P, Bishop WR (2006) Lipid posttranslational modifications. Farnesyl transferase inhibitors. *J Lipid Res* 47:15–31.
9. Rusiñol AE, Sinensky MS (2006) Farnesylated lamins, progeroid syndromes and farnesyl transferase inhibitors. *J Cell Sci* 119:3265–3272.
10. Capell BC, et al. (2008) A farnesyltransferase inhibitor prevents both the onset and late progression of cardiovascular disease in a progeria mouse model. *Proc Natl Acad Sci USA* 105:15902–15907.
11. Yang SH, et al. (2006) A farnesyltransferase inhibitor improves disease phenotypes in mice with a Hutchinson-Gilford progeria syndrome mutation. *J Clin Invest* 116:2115–2121.
12. Kieran MW, et al. (2007) Phase I and pharmacokinetic study of the oral farnesyltransferase inhibitor lonafarnib administered twice daily to pediatric patients with advanced central nervous system tumors using a modified continuous reassessment method: A Pediatric Brain Tumor Consortium Study. *J Clin Oncol* 25:3137–3143.
13. Gordon LB, et al. (2007) Disease progression in Hutchinson-Gilford progeria syndrome: Impact on growth and development. *Pediatrics* 120:824–833.
14. The Progeria Research Foundation International Registry. Available at http://www.progeriaresearch.org/patient_registry.html.
15. Gordon CM, et al. (2011) Hutchinson-Gilford progeria is a skeletal dysplasia. *J Bone Miner Res* 26:1670–1679.
16. Gerhard-Herman M, et al. (2012) Mechanisms of premature vascular aging in children with Hutchinson-Gilford progeria syndrome. *Hypertension* 59:92–97.
17. Wren TA, Liu X, Pitukcheewanont P, Gilsanz V (2005) Bone acquisition in healthy children and adolescents: Comparisons of dual-energy x-ray absorptiometry and computed tomography measures. *J Clin Endocrinol Metab* 90:1925–1928.
18. Schofield WN (1985) Predicting basal metabolic rate, new standards and review of previous work. *Hum Nutr Clin Nutr* 39(Suppl 1):5–41.
19. Reusz GS, et al. (2010) Reference values of pulse wave velocity in healthy children and teenagers. *Hypertension* 56:217–224.
20. Kis E, et al. (2008) Pulse wave velocity in end-stage renal disease: Influence of age and body dimensions. *Pediatr Res* 63:95–98.
21. Feldman EJ, et al. (2008) On the use of lonafarnib in myelodysplastic syndrome and chronic myelomonocytic leukemia. *Leukemia* 22:1707–1711.
22. Domingo DL, et al. (2009) Hutchinson-Gilford progeria syndrome: Oral and craniofacial phenotypes. *Oral Dis* 15:187–195.
23. O'Rourke MF, Staessen JA, Vlachopoulos C, Duprez D, Plante GE (2002) Clinical applications of arterial stiffness; definitions and reference values. *Am J Hypertens* 15:426–444.
24. Redheuil A, et al. (2010) Reduced ascending aortic strain and distensibility: Earliest manifestations of vascular aging in humans. *Hypertension* 55:319–326.
25. Cruickshank K, et al. (2002) Aortic pulse-wave velocity and its relationship to mortality in diabetes and glucose intolerance: An integrated index of vascular function? *Circulation* 106:2085–2090.
26. Varga R, et al. (2006) Progressive vascular smooth muscle cell defects in a mouse model of Hutchinson-Gilford progeria syndrome. *Proc Natl Acad Sci USA* 103:3250–3255.
27. Olive M, et al. (2010) Cardiovascular pathology in Hutchinson-Gilford progeria: Correlation with the vascular pathology of aging. *Arterioscler Thromb Vasc Biol* 30:2301–2309.
28. Lind L, Andersson J, Rönn M, Gustavsson T (2007) The echogenicity of the intima-media complex in the common carotid artery is closely related to the echogenicity in plaques. *Atherosclerosis* 195:411–414.
29. Stehens WE, Delahunt B, Shozawa T, Gilbert-Barnes E (2001) Smooth muscle cell depletion and collagen types in progeric arteries. *Cardiovasc Pathol* 10:133–136.
30. Binkley TL, Berry R, Specker BL (2008) Methods for measurement of pediatric bone. *Rev Endocr Metab Disord* 9:95–106.
31. Bertrand AT, Chikhaoui K, Yaou RB, Bonne G (2011) Clinical and genetic heterogeneity in laminopathies. *Biochem Soc Trans* 39:1687–1692.
32. James GL, Goldstein JL, Brown MS (1995) Polylysine and CVIM sequences of K-RasB dictate specificity of prenylation and confer resistance to benzodiazepine peptidomimetic in vitro. *J Biol Chem* 270:6221–6226.
33. McClintock D, Gordon LB, Djabali K (2006) Hutchinson-Gilford progeria mutant lamin A primarily targets human vascular cells as detected by an anti-Lamin A G608G antibody. *Proc Natl Acad Sci USA* 103:2154–2159.
34. Scaffidi P, Misteli T (2006) Lamin A-dependent nuclear defects in human aging. *Science* 312:1059–1063.
35. McClintock D, et al. (2007) The mutant form of lamin A that causes Hutchinson-Gilford progeria is a biomarker of cellular aging in human skin. *PLoS ONE* 2:e1269.
36. Cao K, et al. (2011) Progerin and telomere dysfunction collaborate to trigger cellular senescence in normal human fibroblasts. *J Clin Invest* 121:2833–2844.
37. Scaffidi P, Gordon L, Misteli T (2005) The cell nucleus and aging: Tantalizing clues and hopeful promises. *PLoS Biol* 3:e395.
38. Fong LG, et al. (2006) A protein farnesyltransferase inhibitor ameliorates disease in a mouse model of progeria. *Science* 311:1621–1623.
39. Gordon CM, et al. (2002) Effects of oral dehydroepiandrosterone on bone density in young women with anorexia nervosa: A randomized trial. *J Clin Endocrinol Metab* 87:4935–4941.
40. Kenna MA, et al. (2010) Audiologic phenotype and progression in GJB2 (Connexin 26) hearing loss. *Arch Otolaryngol Head Neck Surg* 136:81–87.
41. Kuczmarik RJ, et al. (2002) *2000 CDC Growth Charts for the United States: Methods and Development* (National Center for Health Statistics. Vital and Health Statistics, Washington, DC), Series 11, No. 246. Available at <http://www.cdc.gov/growthcharts/2000growthchart-us.pdf>.